# 2HDM benchmarking

P. M. Ferreira,* Rui Santos†

June 18, 2013

## 1 Potential, parameters and constraints

The scalar potential is a softly broken $Z_2$ symmetric 2HDM

$$\begin{aligned} V(\Phi_1,\Phi_2) =& m_1^2\Phi_1^\dagger\Phi_1 + m_2^2\Phi_2^\dagger\Phi_2 + (m_{12}^2\Phi_1^\dagger\Phi_2 + \text{h.c.}) + \frac{1}{2}\lambda_1(\Phi_1^\dagger\Phi_1)^2 + \frac{1}{2}\lambda_2(\Phi_2^\dagger\Phi_2)^2 \\ &+\lambda_3(\Phi_1^\dagger\Phi_1)(\Phi_2^\dagger\Phi_2) + \lambda_4(\Phi_1^\dagger\Phi_2)(\Phi_2^\dagger\Phi_1) + \frac{1}{2}\lambda_5[(\Phi_1^\dagger\Phi_2)^2 + \text{h.c.}] \ , \end{aligned}$$

where $\Phi_i$, $i = 1, 2$ are complex SU(2) doublets. All parameters except for $m_{12}^2$ and $\lambda_5$ are real as a consequence of the hermiticity of the potential. We consider a CP-conserving model at the potential level with $m_{12}^2$, $\lambda_5$ and the vacuum expectation values real. Free parameters are $m_h$, $m_H$, $m_A$, $m_{H^\pm}$, $\tan\beta = v_2/v_1$, $\alpha$ and $m_{12}^2$. We only consider here two of the non-FCNC models known as type I and type II.

We have imposed the following theoretical bounds: we require that the potential is bounded from below and we impose unitarity limits on the quartic Higgs couplings. We have also taken into account the precision electroweak constraints. With the available bounds on the parameters coming mainly from LEP and B-physics, our scans are performed taking $m_{H^\pm} \geq 90$ GeV for type I while $m_{H^\pm} \geq 360$ GeV for type II (upper limit is 600 GeV for both types). We also take $-600^2$ Gev$^2 \leq m_{12}^2 \leq 600^2$ Gev$^2$, 90 GeV $\leq m_A \leq 600$ GeV, $m_h = 125$ GeV, $1 \leq \tan\beta \leq 30$ and 600 GeV $\geq m_H > m_h$ while $\alpha$ is free to vary in its allowed range although subject to the above constraints.

In figure 1 we show the the points in the ($m_{12}^2$, $\tan\beta$) plane that passed all theoretical and experimental constraints for model type II (similar results for type I regarding the high $\tan\beta$ behaviour). The zoom presented on the left shows agreement with the points presented by Rompotis, Goussiou (+Stal and Harlander) on May 15. We note however that there are a lot of points passing all the constraints for high $\tan\beta$. Moreover, we are now generating points with $\tan\beta > 15$ to fill the region where $\tan\beta$ is large.

## 2 Benchmarking

We have not been following the discussion on 2HDM benchmarking from the beginning. So we would like to discuss why we need benchmarking from the experimental point of view. I see at least two problems we need to address. One is the gluon fusion production process where the distributions change for high $\tan\beta$ due to the b-quark contributions. This I believe was

*E-mail: ferreira@cii.fc.ul.pt
†E-mail: rsantos@cii.fc.ul.pt

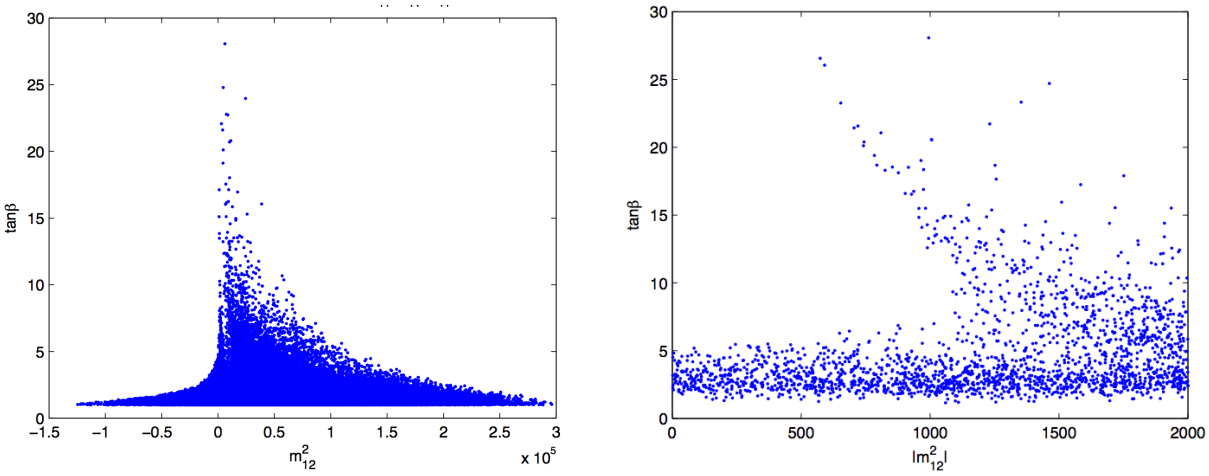


Figure 1: Left - points in the $(m_{12}^2, \tan\beta)$ plane that passed all theoretical and experimental constraints. Right- zoom in the region where $\tan\beta$ is large.

discussed in the previous meeting. The second is the total width of the scalar which will have an impact on the limits extracted from data.

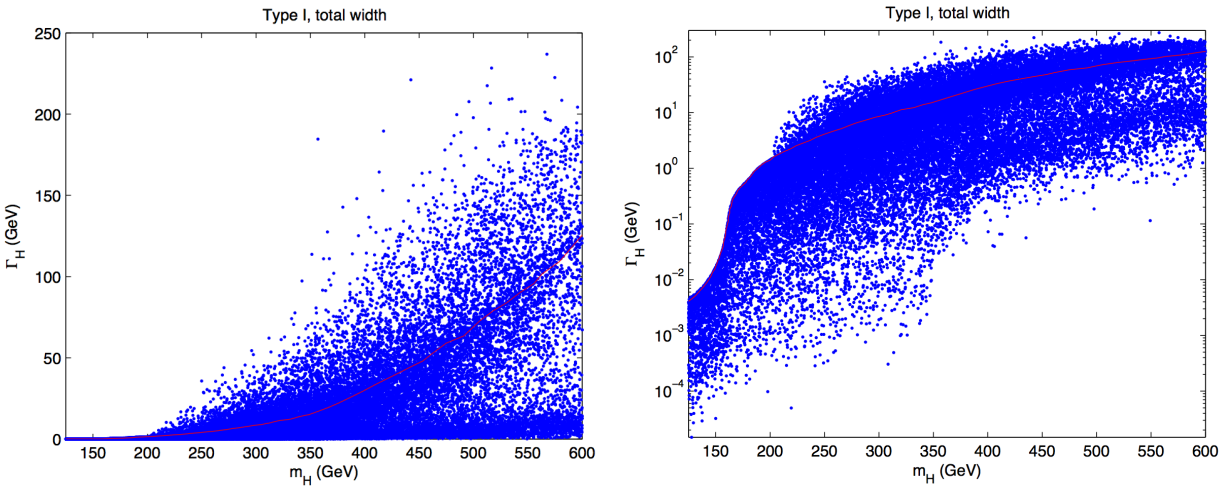


Figure 2: Total width of $H$ as a function of $m_H$ for type I with all constraints. Red line is the total width for a "SM Higgs" boson. Right: same plot but with log scale on width axis.

In figure 2 we present the total width for $H$ as a function of $m_H$ for the type I model with all constraints described above. We also show the "SM Higgs" boson width (red line). The allowed values are scattered around the red line. Therefore it seems that we should build a grid where the experimental analysis would be performed. That way we would cover "all" parameter space of the 2HDM. Let me clarify here that by grid I mean some points in the $(m_H, \Gamma_H)$ plane that would cover most of the 2HDM parameter space. Each point on this grid would have one (or many) correspondent points in parameter space that could be used as benchmark points.

In figure 3 we present the total width for $H$ as a function of $m_H$ for the type II model, again with all constraints described above. We again show the "SM Higgs" boson width (red line). In

figure 4 we show the $\Gamma(H \to ZZ)$ for the type I (left) and type II (right) as a function of $m_H$.

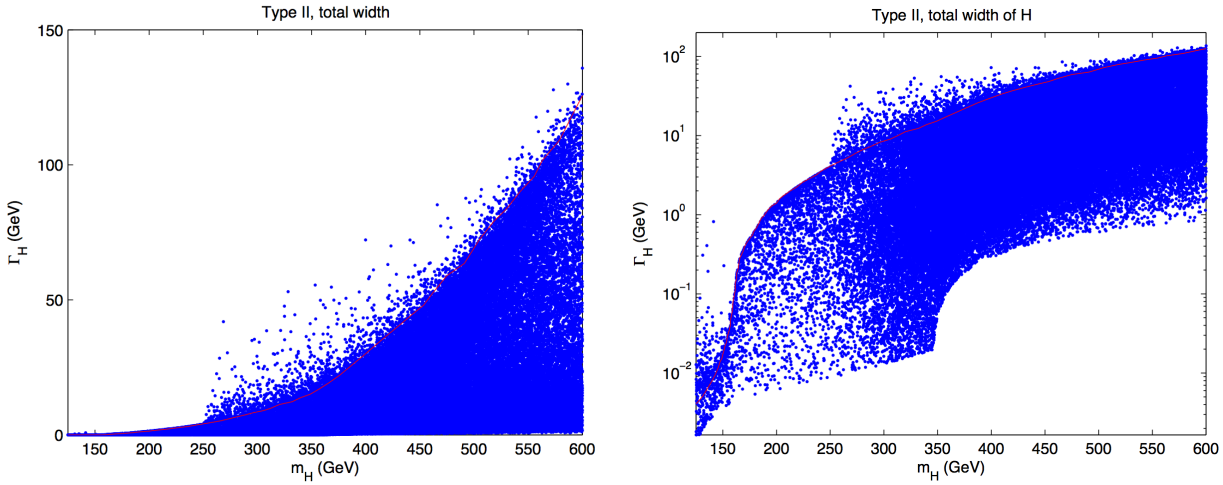


Figure 3: Total width of $H$ as a function of $m_H$ for the type II with all constraints. Red line is the total width for a "SM Higgs" boson. Right: same plot but with log scale on width axis.

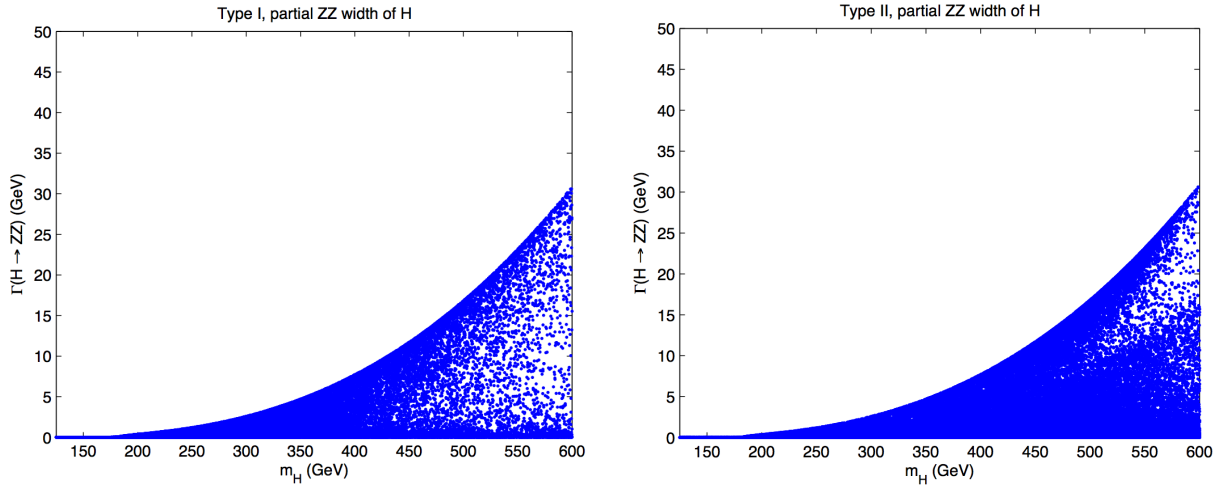


Figure 4: $\Gamma(H \to ZZ)$ for the type I (left) and type II (right) as a function of $m_H$.

## 3 Bounds from the lightest scalar analysis

The heavier CP-even scalar couples to the gauge bosons as $g_{SM}\cos(\beta-\alpha)$. There are already bounds on the $(\cos(\beta-\alpha), \tan\beta)$ from the data on the 125 GeV Higgs. This is shown in figure 5 where we present the points in the $(\cos(\beta-\alpha), \tan\beta)$ plane that passed all the constraints in type II using the ATLAS data (left) and using the CMS data (right) at $1\sigma$ in green (light grey) and $2\sigma$ in blue (dark grey) (experimental results presented at Moriond). Also shown are the lines for the SM-like limit, that is $\cos(\beta-\alpha)=0$ and for the limit $\cos(\beta+\alpha)=0$ (see [1] for details).

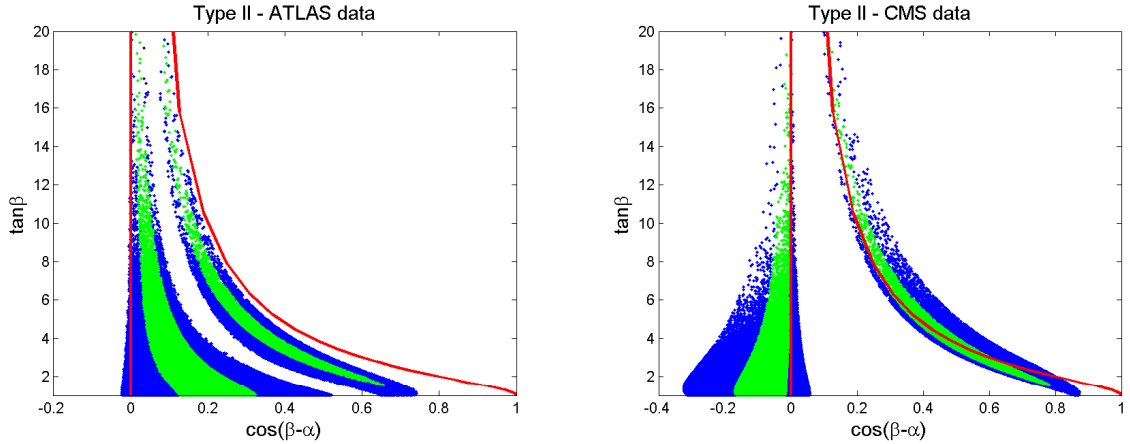


Figure 5: Points in the $(\cos(\beta-\alpha), \tan\beta)$ plane that passed all the constraints in type II using the ATLAS data (left) and using the CMS data (right) at $1\sigma$ in green (light grey) and $2\sigma$ in blue (dark grey). Also shown are the lines for the SM-like limit, that is $\cos(\beta-\alpha)=0$ and for the limit $\cos(\beta+\alpha)=0$.

# 4 New plots 12/06/2013

We have generated a new set of points (10900) with $\tan\beta > 10$ and we have also increased the upper bound to all masses (except of course for the 125 GeV Higgs) to 800 GeV. The results are shown in figure 6 where on the left we plot the points in the $(m_H, \tan\beta)$ plane (that passed all theoretical and experimental constraints) and on the right we plot the points in the $(m_{12}^2, \tan\beta)$ plane. It is clear that there are large values of $\tan\beta$ for the entire range of $m_H$. There is a concentration of points around 400 GeV that is related to the bound on the charged Higgs mass and arises via electroweak constraints. In type I the points are concentrated closer to the smaller masses. In the right panel we show $(m_{12}^2, \tan\beta)$ for different ranges of $m_H$ (in the plot all masses mean $m_H = m_A = m_{H^\pm}$).

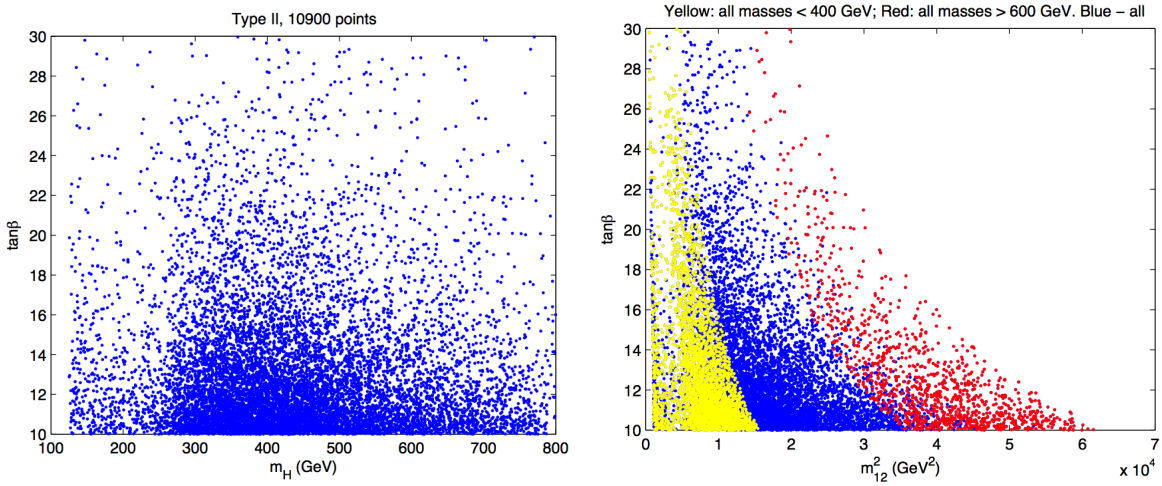


Figure 6: Left - points in the $(m_H, \tan\beta)$ plane that passed all theoretical and experimental constraints. Right- same in $(m_{12}^2, \tan\beta)$ plane.

In figure 7 we present the points that passed all theoretical and experimental constraints in the $(m_{12}^2, \tan\beta)$ plane with $m_h = 125$ GeV, $m_H = m_A = m_{H^\pm} = 130$ GeV and $\alpha$ free.

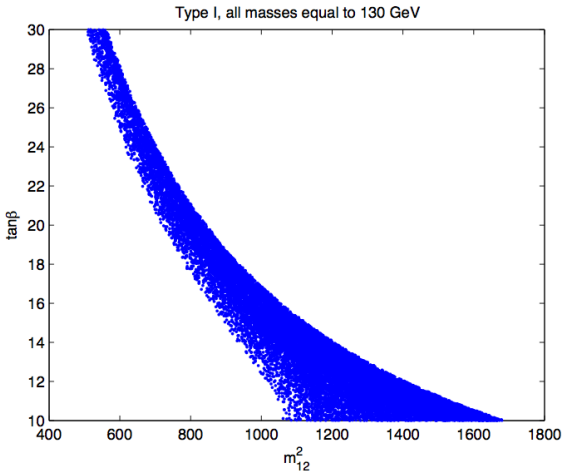


Figure 7: Points in the $(m_{12}^2, \tan\beta)$ plane that passed all theoretical and experimental constraints with $m_h = 125$ GeV, $m_H = m_A = m_{H^\pm} = 130$ GeV and $\alpha$ free.

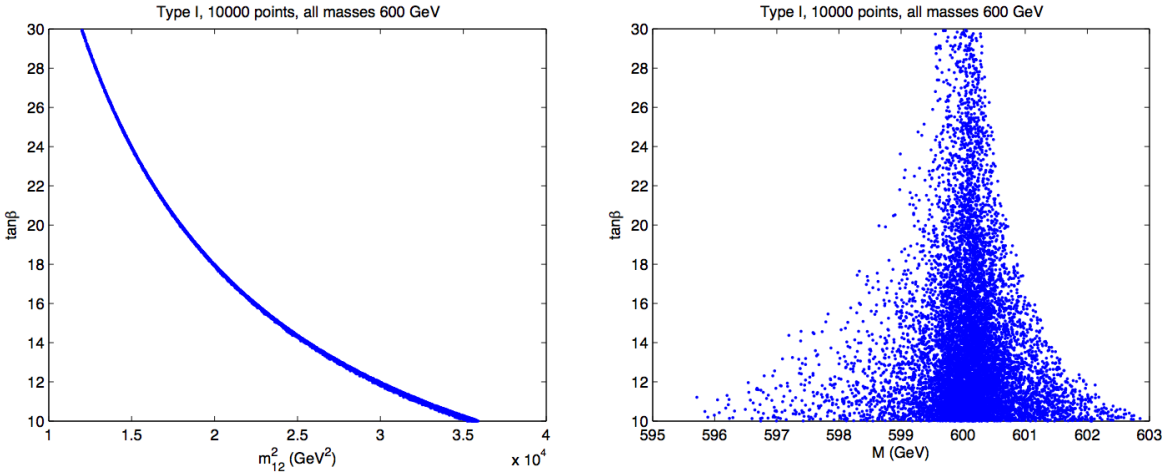


Figure 8: Left - points in the $(m_{12}^2, \tan\beta)$ plane that passed all theoretical and experimental constraints with $m_h = 125$ GeV, $m_H = m_A = m_{H^\pm} = 600$ GeV and $\alpha$ free. Right- same in $(M, \tan\beta)$ plane.

In figure 8 we present the points that passed all theoretical and experimental constraints in the $(m_{12}^2, \tan\beta)$ plane (left) and in the $(M, \tan\beta)$ plane (right) for type I with $m_h = 125$ GeV, $m_H = m_A = m_{H^\pm} = 600$ GeV and $\alpha$ free. $M$ is defined as $M^2 = m_{12}^2/(\sin\beta\cos\beta)$. When $M = m_H = m_A = m_{H^\pm}$ and large (decoupling), $\sin(\beta-\alpha) \to 1$ and the larger $\tan\beta$ the closer to 1 $\sin(\beta-\alpha)$ is. This is shown in figure 9. Note in figure 8 (right) that the values of $M$ concentrate around 600 GeV which are the common values for $m_H = m_A = m_{H^\pm}$. To go to very large $\tan\beta$ we always have to take $M$ close to the mass of the heavy scalars. If $M = 0$ and $m_h = 125$ GeV a limit of $\tan\beta < 6$ was derived in [2].

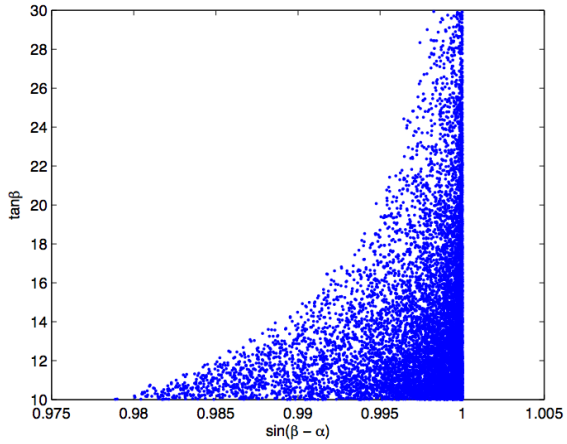


Figure 9: Points in the $(\sin(\beta-\alpha), \tan\beta)$ plane that passed all theoretical and experimental constraints with $m_h = 125$ GeV, $m_H = m_A = m_{H^\pm} = 600$ GeV and $\alpha$ free.

## 5 New plots 17/06/2013

In figure 10 we show points in the $(\sin(\beta-\alpha), m_H)$ plane that passed all theoretical and experimental constraints with $m_h = 125$ GeV and all other parameters free. Left - type I. Right- type II. The difference between the two plots is just that in type II the mass of the charged Higgs is above 360 GeV. Green points have $8 < \tan\beta < 15$ and red points have $\tan\beta > 15$.

In figure 11 we have generated a new set of points with $\tan\beta > 5$, $m_H = 600$ GeV and $m_h = 125$ GeV and all other parameters free. Points are for type I and are plotted in the $(\sin(\beta-\alpha), \tan\beta)$ plane. The red points (which are on top of the blue points) are for a charged Higgs mass above 360 GeV.

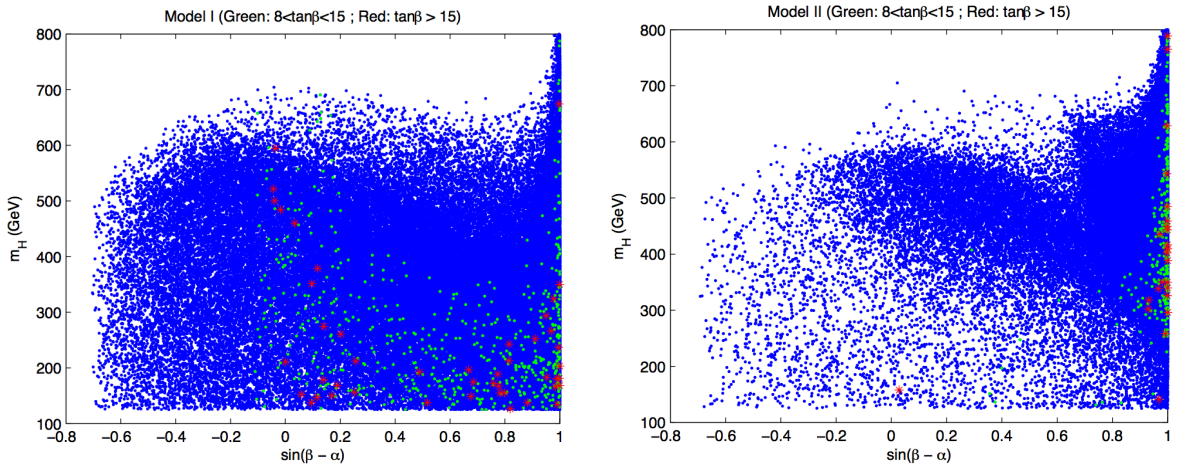


Figure 10: Points in the $(\sin(\beta-\alpha), \tan\beta)$ plane that passed all theoretical and experimental constraints with $m_h = 125$ GeV and all other parameters free. Left - type I. Right- type II.

Considering all the plots we can conclude:

- There is a wide range of allowed values of $\sin(\beta-\alpha)$ for $m_H$ below 700 GeV. For larger $m_H$, $\sin(\beta-\alpha)$ is close to 1.
- In type I, the charged Higgs can be light. This means that electroweak constraints can be

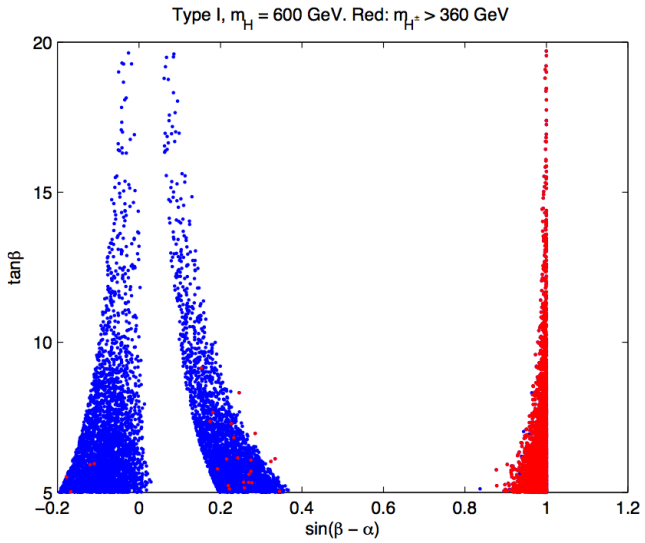


Figure 11: Points in the $(\sin(\beta-\alpha), \tan\beta)$ plane that passed all theoretical and experimental constraints with $m_h = 125$ GeV, $m_H = 600$ GeV and the remaining parameters free.

evaded for a charged Higgs mass close to $m_h$ AND $\sin(\beta-\alpha)$ close to zero. That is why in type II there are almost no green and red points.

- However (figure 11) taking $\tan\beta > 5$ we see that the allowed regions for $\sin(\beta-\alpha)$ between -0.2 and 0.4 are already excluded by the results for $m_h = 125$ GeV (figure 12) .

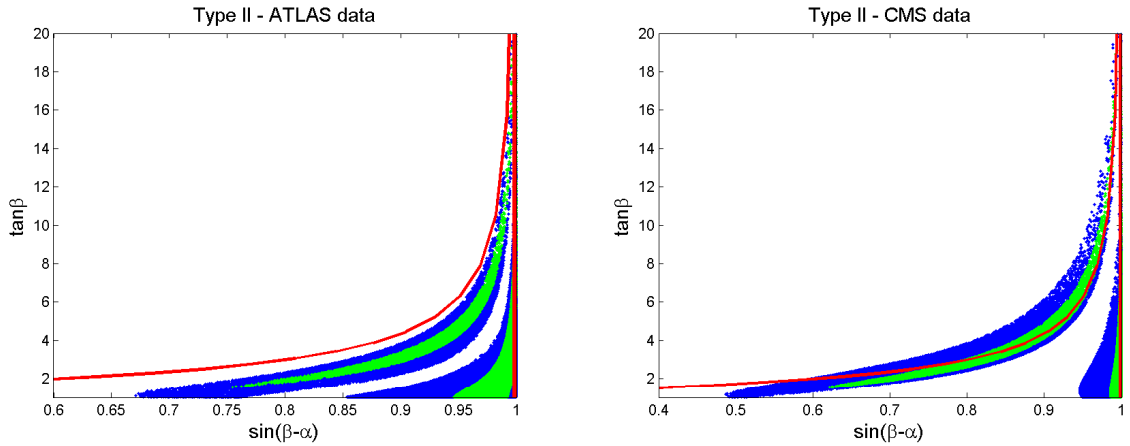


Figure 12: Points in the $(\sin(\beta-\alpha), \tan\beta)$ plane that passed all the constraints in type II using the ATLAS data (left) and using the CMS data (right) at $1\sigma$ in green (light grey) and $2\sigma$ in blue (dark grey). Also shown are the lines for the SM-like limit, that is $\sin(\beta-\alpha) = 1$ and for the limit $\sin(\beta+\alpha) = 1$.

## References

[1] A. Barroso, P. M. Ferreira, R. Santos, M. Sher and J. P. Silva, arXiv:1304.5225 [hep-ph]; P. M. Ferreira, R. Santos, M. Sher and J. P. Silva, arXiv:1305.4587 [hep-ph].

[2] B. Gorczyca, M. Krawczyk and , arXiv:1112.5086 [hep-ph].